Journal of Computational and Applied Mathematics 341 (2018) 117–126

Contents lists available at ScienceDirect

Journal of Computational and Applied Mathematics

journal homepage: www.elsevier.com/locate/cam

Sequence of G^n LN polynomial curves approximating circular arcs

Young Joon Ahn [a,*], Christoph Hoffmann [b]

[a] Department of Mathematics Education, Chosun University, Gwangju, 501–759, South Korea
[b] Department of Computer Science, Purdue University, West Lafayette, IN 47907, USA

ARTICLE INFO

Article history:
Received 5 April 2017
Received in revised form 9 December 2017

Keywords:
Circle approximation
Ellipse approximation
Linear normal curve
Hausdorff distance
G^n endpoint interpolation

ABSTRACT

In this paper we derive a sequence of linear normal (LN) curves $\mathbf{b}_{2n}$ of degree $2n$ which are G^n endpoint interpolations of a circular arc and have approximation order $2n+2$. This is an extension of the circle approximation method by LN Bézier curves given in Ahn and Hoffmann (2014) to all even degrees. We also extend the circle approximation to an ellipse approximation by G^n LN curves of degree $2n$. An upper bound of the Hausdorff distance between the ellipse and its LN approximation is obtained. We illustrate our results through an LN approximation of convolution curves of ellipses and a spline curve.

1. Introduction

Circle approximation methods using polynomial curves with high accuracy have been developed for the last thirty years [1–3]. First, de Boor proposed the approximation of planar curves, including circles, using cubic Bézier curves. His method achieved an approximation order of six [1]. Later, a number of circle or conic approximation methods using nth degree Bézier curves were presented. They achieved an approximation order of $2n$, with various orders of geometric continuity G^k, where $2 \le n \le 5$ and $1 \le k \le n-1$ [2–11]. Remarkably, this development included Floater's conic approximations by G^2 quadratic curves and by G^{n-1} polynomial curves of all odd degrees n, achieving an approximation order of $2n$ [12,13].

Circle approximation using LN (linear normal) curves could play an important role in the field of offset approximation, since an offset approximation method based on circle approximation by quadratic Bézier curves was presented by Lee et al. [14]. The quadratic Bézier curve is an LN curve of minimum degree and so it has a rational offset [15,16]. An LN surface was first devised in order to obtain rational offset surfaces [17]. Several methods of circle approximation using LN curves with continuous curvature have been proposed in [18–20]. In particular, circle approximations using G^n LN Bézier curves of degree $2n = 4$ or 6 were presented in [18]. The motivation of this paper is to generalize circle approximation by G^n LN curves to all even degrees.

In this paper we construct a sequence of LN polynomial curves of even degree $2n$ which are G^n endpoint interpolations of circular arcs. Furthermore, we extend this G^n LN circle approximation to a G^n LN ellipse approximation. Using the formula for sequences of LN polynomial curves, we obtain the exact Hausdorff distance between the ellipse and LN polynomial curves and the approximation order $2n$. Our results can be applied to offset approximation and to the approximation of convolutions of spline curves and ellipses.

The remainder of this paper is organized as follows. In Section 2, some basic facts concerning circle approximation by polynomial curves are presented. In Section 3, the sequence of LN polynomial curves which are G^n endpoint interpolations of circular arcs is presented, and the Hausdorff distance and its approximation order are obtained. In Section 4, an extension

* Corresponding author.
E-mail address: kaistahn@daum.net (Y.J. Ahn).

https://doi.org/10.1016/j.cam.2018.03.028
0377-0427/

of the G^n LN circle approximation to a G^n LN ellipse approximation is devised. In Section 5, we compare our method to previous conic approximation methods, and in Section 6 an example is constructed that illustrates our method of LN ellipse approximation through the approximation of font outlines defined by sweeping an ellipse along a spline curve. In Section 7, we summarize our results.

2. Preliminaries for circle approximation

Let $\mathbf{c}$ be a circular arc subtending the angle $2\alpha < \pi$,

$$\mathbf{c}(\theta) = (\cos(\theta), \sin(\theta)), \qquad \theta \in [-\alpha, \alpha], \tag{1}$$

and $\mathbf{b}_{2n}$ be a polynomial plane curve of degree $2n$,

$$\mathbf{b}_{2n}(t) = (x_{2n}(t), y_{2n}(t)), \qquad t \in [0, 1],$$

which is the approximation curve of the circular arc.

The Hausdorff distance between the circular arc $\mathbf{c}$ and its approximation curve $\mathbf{b}_{2n}$ is

$$d_H(\mathbf{c}, \mathbf{b}_{2n}) = \max_{t\in[0,1]} |\phi(t)|$$

where $\phi(t) = \sqrt{x_{2n}(t)^2 + y_{2n}(t)^2} - 1$, if the argument of the complex number $x_{2n}(t) + iy_{2n}(t)$ is contained in $[-\alpha, \alpha]$ for all $t \in [0, 1]$. The irrational function $\phi(t)$ and the polynomial

$$\psi(t) = x_{2n}(t)^2 + y_{2n}(t)^2 - 1$$

have the same points satisfying $\phi'(t) = \psi'(t) = 0$. Since circular arcs are symmetric, it is suitable that the approximation curve $\mathbf{b}_{2n}$ is too. Thus $x_{2n}(1-t) = x_{2n}(t)$, $y_{2n}(1-t) = -y_{2n}(t)$, and

$$d_H(\mathbf{c}, \mathbf{b}_{2n}) = \begin{cases} \sqrt{\psi_+ + 1} - 1 & (\psi_+ \geq \psi_-) \\ 1 - \sqrt{1 - \psi_-} & (\psi_+ < \psi_-) \end{cases}$$

where $\psi_+ = \max_{t\in[0,\frac{1}{2}]}\psi(t)$ and $\psi_- = -\min_{t\in[0,\frac{1}{2}]}\psi(t)$.

It is well-known [6,21] that for $n \geq 1$ the approximate curve $\mathbf{b}_{2n}$ of even degree $2n$ is a G^n endpoint interpolation of a circular arc $\mathbf{c}(\theta)$ if

$$\begin{aligned} \mathbf{c}'(-\alpha) \cdot \mathbf{b}'_{2n}(0) &> 0 \\ \left.\frac{d^i\psi(t)}{dt^i}\right|_{t=0} &= 0, \qquad i = 0, \ldots, n. \end{aligned} \tag{2}$$

Furthermore, the approximation curve $\mathbf{b}_{2n}$ is a linear normal curve if and only if

$$\mathbf{b}'_{2n}(t) \cdot ((1-t)\mathbf{n}(0) + t\mathbf{n}(1)) = 0 \tag{3}$$

for all $t \in [0, 1]$, where $\mathbf{n}(t)$ is the rotation of $\mathbf{b}'_{2n}(t)$ by $\frac{\pi}{2}$, and $\cdot$ is the inner product [22].

Thus, by solving Eqs. (2)–(3) for $n = 2, 3$, Ahn and Hoffmann [18] provided the G^n LN circle approximation $\mathbf{b}_{2n}(t) = \sum_{i=0}^{2n}\mathbf{b}_{i,2n}B_i^{2n}(t)$ with the control points

$$\begin{aligned}
\mathbf{b}_{0,2n} &= (\cos\alpha, -\sin\alpha), \qquad \text{for } n = 2, 3 \\
\mathbf{b}_{1,4} &= \frac{1}{2}\left(\cos\alpha(3-\cos\alpha), -\sin\alpha(1+\sin^2\alpha)\right) \\
\mathbf{b}_{2,4} &= \frac{1}{3}\left(\frac{3-\cos^2\alpha+\cos^4\alpha}{\cos\alpha}, 0\right) \\
\mathbf{b}_{1,6} &= \frac{1}{3}\left(\cos\alpha(4-\cos\alpha), -\sin\alpha(2+\sin^2\alpha)\right) \\
\mathbf{b}_{2,6} &= \frac{1}{15}\left(29-20\cos^2\alpha+6\cos^4\alpha, -\sin\alpha(5+4\sin^2\alpha+6\sin^4\alpha)\right) \\
\mathbf{b}_{3,6} &= \frac{1}{5}\left(\frac{5-\cos^2\alpha+6\cos^4\alpha-2\cos^6\alpha}{\cos\alpha}, 0\right) \\
\mathbf{b}_{i,2n} &= R_x\mathbf{b}_{2n-i,2n} \qquad \text{for } n = 2, 3, \text{ and } n+1 \leq i \leq 2n
\end{aligned}$$

where $B_i^n(t) = \frac{n!}{i!(n-i)!}t^i(1-t)^{n-i}$ and R_x is the reflection operator with respect to the x-axis. In this paper we extend the formula $\mathbf{b}_{2n}(t) = (x_{2n}(t), y_{2n}(t))$ to all $n \in \mathbb{N}$.

3. Circle approximation by G^n LN curves of degree $2n$

In this section we present the sequence of G^n LN circle approximation curves $\mathbf{b}_{2n}(t)$ of degree $2n$ for $n = 1, 2, \ldots$. By solving Eqs. (2)–(3) degree by degree, the formulas for the LN G^n approximation curve $\mathbf{b}_{2n}$ can be obtained as follows:

$$\begin{aligned}
x_2(t) &= \sec\alpha + \sin\alpha\tan\alpha\{2t(1-t) - 1\} \\
y_2(t) &= \sin\alpha(2t-1) \\
x_4(t) &= \sec\alpha + \sin\alpha\tan\alpha\{2t(1-t) - 1 + \sin^2\alpha(6t^2(1-t)^2 - 2t(1-t))\} \\
y_4(t) &= \sin\alpha(2t-1)\{1 + 2(\sin^2\alpha)t(1-t)\} \\
x_6(t) &= \sec\alpha + \sin\alpha\tan\alpha\{2t(1-t) - 1 + \sin^2\alpha(6t^2(1-t)^2 - 2t(1-t)) \\
&\quad + \sin^4\alpha(20t^3(1-t)^3 - 6t^2(1-t)^2)\} \\
y_6(t) &= \sin\alpha(2t-1)\{1 + 2(\sin^2\alpha)t(1-t) + 6(\sin^4\alpha)t^2(1-t)^2\} \\
&\ \ \vdots\ .
\end{aligned}$$

From the list of formulas $\mathbf{b}_{2n}$ for higher degree, we can guess the generalized formula for $\mathbf{b}_{2n}$ for all even degrees as follows:

$$x_{2n}(t) = \sec\alpha + \sin\alpha\tan\alpha\sum_{i=0}^{n-1}\xi_i(t) \tag{4}$$

$$y_{2n}(t) = \sin\alpha\sum_{i=0}^{n-1}\eta_i(t) \tag{5}$$

for $t \in [0, 1]$, where

$$\begin{aligned}
\gamma_n(t) &= \binom{2n}{n} t^n(1-t)^n \\
\xi_n(t) &= (\sin\alpha)^{2n}(\gamma_{n+1}(t) - \gamma_n(t)) \\
\eta_n(t) &= (\sin\alpha)^{2n}(2t-1)\gamma_n(t)
\end{aligned}$$

for $n = 0, 1, \ldots$. Now, we show that all polynomial curves $\mathbf{b}_{2n}(t)$ are linear normal and G^n endpoint interpolations of the circular arc, and we present an upper bound of the Hausdorff distance between the circular arc and $\mathbf{b}_{2n}$, so that its approximation order $n + 2$ can be obtained.

Proposition 3.1. *The curve $\mathbf{b}_{2n}$ is a linear normal curve.*

Proof. Since $\xi_n'(t) = -(\sin\alpha)^{2n}(2t-1)\mu_n(t)$ and $\eta_n'(t) = (\sin\alpha)^{2n}\mu_n(t)$ where

$$\mu_n(t) = \frac{(n+1)\gamma_{n+1}(t) - n\gamma_n(t)}{t(1-t)}$$

for $n = 0, 1, \ldots$, we have that

$$\mathbf{b}_{2n}{}'(t) = \sum_{i=0}^{n-1}(\sin\alpha)^{2i+1}\mu_i(t)\,(-\tan\alpha(2t-1), 1) \tag{6}$$

and so $\mathbf{b}_{2n}$ is a linear normal curve. □

Proposition 3.2. *The curve $\mathbf{b}_{2n}$ is a G^n endpoint interpolation of the circular arc* $\mathbf{c}$.

Proof. Eqs. (4)–(5) yield that $\psi(i) = x_{2n}(i)^2 + y_{2n}(i)^2 - 1 = 0$ for $i = 0, 1$ and for all positive integers n. Since $\psi'(t) = 2(x_{2n}(t)x_{2n}'(t) + y_{2n}(t)y_{2n}'(t))$, Eq. (6) yields that

$$\psi'(t) = 2\left(-\sin\alpha\tan\alpha(2t-1)x_{2n}(t) + \sin\alpha\ y_{2n}(t)\right)\left(\sum_{i=0}^{n-1}(\sin\alpha)^{2i}\mu_i(t)\right).$$

For all positive integers n, it holds that

$$\begin{aligned}
&-\sin\alpha\tan\alpha(2t-1)x_{2n}(t) + \sin\alpha\ y_{2n}(t) \\
&= -(\tan\alpha)^2(2t-1)\left[1 + \sum_{i=0}^{n-1}\left\{(\sin\alpha)^{2i+2}\gamma_{i+1}(t) - (\sin\alpha)^{2i}\gamma_i(t)\right\}\right].
\end{aligned}$$

This sum is telescoping, and so

$$\psi'(t)=2\binom{2n}{n}(\sin\alpha)^{2n}(\tan\alpha)^2t^n(1-t)^n(2t-1)\left(\sum_{i=0}^{n-1}(\sin\alpha)^{2i}\mu_i(t)\right). \quad (7)$$

Therefore, $\left.\frac{d^i\psi(t)}{dt^i}\right|_{t=0,1}=0$ for $i=0,1,\ldots,n$, and so the curve $\mathbf{b}_{2n}$ is a G^n endpoint interpolation of the circular arc $\mathbf{c}$. □

Lemma 3.3. *For all positive integers n,*

$$\sum_{i=0}^{n-1}(\sin\alpha)^{2i}\mu_i(t)>0$$

in the closed interval $[0,1]$.

Proof. Since $\mu_n(t)$ is a function of $t(1-t)$ for $n=0,1,\ldots$, using the transformation $s=t(1-t)$, we obtain

$$\mu_n(t)=\mu_n^*(s)=\binom{2n}{n}s^{n-1}\{(4n+2)s-n\}$$

for $s\in[0,\frac{1}{4}]$. $\mu_0^*(s)\equiv 2$. Put $s_0=0$ and $s_n=\frac{n}{4n+2}$, $n=1,2,\ldots$. For all positive integers n, $\mu_n^*(s)$ has a unique zero at s_n in the open interval $(0,\frac{1}{4})$, and $\mu_n^*(s)\le 0$ in $[0,s_n]$ and $\mu_n^*(s)\ge 0$ in $[s_n,\frac{1}{4}]$. For all positive integers n and for all $k=1,\ldots,n-1$, in the interval $[s_{k-1},s_k]$

$$\mu_i^*(s)\begin{cases}\ge 0 & (1\le i\le k-1)\\ \le 0 & (k\le i\le n-1)\end{cases}$$

and in the interval $[s_{n-1},\frac{1}{4}]$, $\mu_i^*(s)\ge 0$ for $i=1,\ldots,n$. Thus in the interval $[s_{k-1},s_k]$, $k=1,\ldots,n-1$, we have that

$$\begin{aligned}\sum_{i=0}^{n-1}(\sin\alpha)^{2i}\mu_i^*(s)&=\sum_{i=0}^{k-1}(\sin\alpha)^{2i}\mu_i^*(s)+\sum_{i=k}^{n-1}(\sin\alpha)^{2i}\mu_i^*(s)\\&>\sum_{i=0}^{k-1}(\sin\alpha)^{2k}\mu_i^*(s)+\sum_{i=k}^{n-1}(\sin\alpha)^{2k}\mu_i^*(s)\\&=(\sin\alpha)^{2k}\sum_{i=0}^{n-1}\mu_i^*(s)=(\sin\alpha)^{2k}n\binom{2n}{n}s^{n-1}\ge 0\end{aligned}$$

by the telescoping sum. In the interval $[s_{n-1},\frac{1}{4}]$, it holds that

$$\sum_{i=0}^{n-1}(\sin\alpha)^{2i}\mu_i^*(s)=2+\sum_{i=1}^{n-1}(\sin\alpha)^{2i}\mu_i^*(s)\ge 2.$$

Therefore, $\sum_{i=0}^{n-1}(\sin\alpha)^{2i}\mu_i^*(s)>0$ in $[0,\frac{1}{4}]$, and so $\sum_{i=0}^{n-1}(\sin\alpha)^{2i}\mu_i(t)>0$ in $[0,1]$. □

Proposition 3.4. *For all positive integers n, the curve* $\mathbf{b}_{2n}$ *lies outside of the circular arc* $\mathbf{c}$ *and the Hausdorff distance between* $\mathbf{c}$ *and* $\mathbf{b}_{2n}$ *is*

$$d_H(\mathbf{c},\mathbf{b}_{2n})=\frac{1}{\cos\alpha}\left\{1-\cos\alpha-\sum_{i=0}^{n-1}\frac{\binom{2i}{i}}{2^{2i+1}(i+1)}(\sin\alpha)^{2i+2}\right\}. \quad (8)$$

Its approximation order is $2n+2$.

Proof. By Eq. (6) and Lemma 3.3, $x_{2n}(t)$ is increasing in the interval $[0,\frac{1}{2}]$ and decreasing in $[\frac{1}{2},1]$, and $y_{2n}(t)$ is increasing in $[0,1]$. Thus, for all positive integers n the continuous curve $\mathbf{b}_{2n}$ lies inside a (closed) rectangle

$$[x(0),x(1/2)]\times[y(0),y(1)]$$

in the xy-plane. By Eq. (7) and Lemma 3.3, $\psi(t)$ is increasing in $[0,\frac{1}{2}]$ and decreasing in $[\frac{1}{2},1]$. Thus $\max_{t\in[0,1]}|\psi(t)|=\psi(\frac{1}{2})$, $\psi(t)>0$ for all $t\in(0,1)$, and $\mathbf{b}_{2n}$ lies outside of the circular arc $\mathbf{c}$. Since $d_H(\mathbf{c},\mathbf{b}_{2n})=x_{2n}(\frac{1}{2})-1$ and

$$x_{2n}(1/2)=\frac{1}{\cos\alpha}\{1-\sum_{i=0}^{n-1}\frac{\binom{2i}{i}}{2^{2i+1}(i+1)}(\sin\alpha)^{2i+2}\},$$

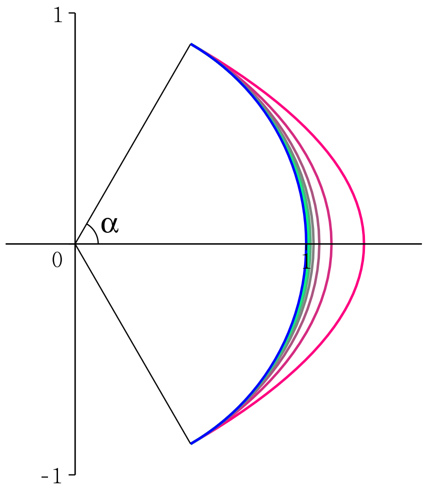

Fig. 1. G^n LN approximation of degree $2n$ of the circular arc (blue) of angle $2\alpha = \frac{\pi}{3}$ for $n = 1, 2, \ldots, 7$ (from red to green). (For interpretation of the references to color in this figure legend, the reader is referred to the web version of this article.)

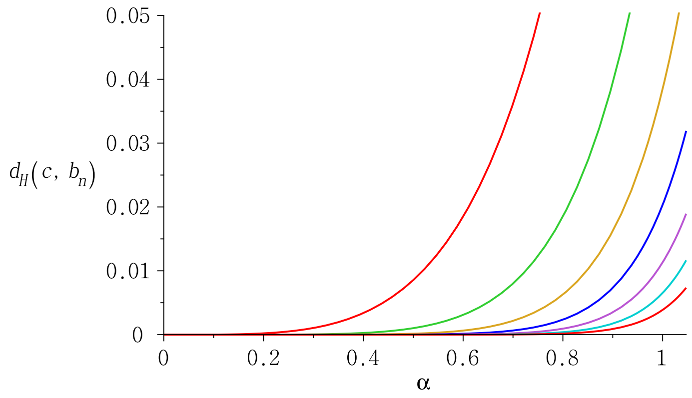

Fig. 2. $d_H(\mathbf{c}, \mathbf{b}_{2n})$ for $\alpha \in (0, \pi/4]$, $n = 1, 2, \ldots, 7$ (from top to bottom).

Eq. (8) follows. Using Taylor series expansion

$$1 - \sqrt{1 - x^2} = \sum_{n=0}^{\infty} \frac{\binom{2n}{n}}{2^{2n+1}(n+1)} x^{2n+2}$$

for $x \in (-1, 1)$, we have that

$$d_H(\mathbf{c}, \mathbf{b}_{2n}) = \frac{\binom{2n}{n}}{2^{2n+1}(n+1)} \alpha^{2n+2} + \mathcal{O}(\alpha^{2n+4})$$

and so the approximation order is $2n + 2$. □

Fig. 1 shows the LN curves $\mathbf{b}_{2n}$ of degree $2n$ for $n = 1, 2, \ldots, 7$ which are G^n endpoint interpolations of the circular arc of angle $2\alpha = \frac{\pi}{3}$. The graphs of the Hausdorff distances $d_H(\mathbf{c}, \mathbf{b}_{2n})$ between the circular arc $\mathbf{c}$ of angle $\alpha \in (0, \pi/4]$ and its G^n LN approximation curves $\mathbf{b}_{2n}$, $n = 1, 2, \ldots, 7$, are presented in Fig. 2. The sequence of G^n LN circle approximations of degree $2n$ is extended to one for ellipse approximations in the following section.

4. Extension to ellipse approximations by LN curves

In this section, we find a sequence of LN curves of degree $2n$ which are G^n endpoint interpolations of an ellipse. A conic $\mathbf{r}$ is represented in the standard rational quadratic Bézier form as

$$\mathbf{r}(t) = \frac{\mathbf{p}_0 B_0^2(t) + w\mathbf{p}_1 B_1^2(t) + \mathbf{p}_2 B_2^2(t)}{B_0^2(t) + w B_1^2(t) + B_2^2(t)}$$

where the conic $\mathbf{r}$ has the control points $\mathbf{p}_0$, $\mathbf{p}_1$, $\mathbf{p}_2$ and the weights $1, w, 1$. We extend the sequence of LN circle approximation to that of LN conic approximation by

$$\mathbf{b}_{2n}(t) = \sum_{j=0}^{2} \tau_{j,n}(t)\mathbf{p}_j \tag{9}$$

with

$$\tau_{0,n}(t) = \sum_{i=0}^{n-1} \lambda_{0,i}(t), \quad \tau_{1,n}(t) = 1 - \sum_{i=0}^{n-1} \lambda_{1,i}(t), \quad \tau_{2,n}(t) = \sum_{i=0}^{n-1} \lambda_{2,i}(t) \tag{10}$$

for positive integers $n \geq 1$, where

$$\begin{aligned} \lambda_{0,n}(t) &= \frac{(\sin\alpha)^{2n}(1-t)}{2(n+1)t}\{(n+1)\gamma_{n+1}(t) - 2nt\gamma_n(t)\} \\ \lambda_{1,n}(t) &= -(\sin\alpha)^{2n}(\gamma_{n+1}(t) - \gamma_n(t)) \\ \lambda_{2,n}(t) &= \frac{(\sin\alpha)^{2n}t}{2(n+1)(1-t)}\{(n+1)\gamma_{n+1}(t) - 2n(1-t)\gamma_n(t)\} \end{aligned} \tag{11}$$

for nonnegative integers $n \geq 0$. This extension in Eq. (10) is inferred from Eqs. (4)–(5) using an affine transformation from the $\tau_0\tau_2$-plane to the xy-plane mapping a triangle with vertices $(0, 0), (1, 0), (0, 1)$ to one with vertices $(\sec\alpha, 0), (\cos\alpha, -\sin\alpha), (\cos\alpha, \sin\alpha)$, i.e.,

$$\begin{pmatrix} x \\ y \end{pmatrix} = \sin\alpha \begin{pmatrix} -\tan\alpha & -\tan\alpha \\ -1 & 1 \end{pmatrix} \begin{pmatrix} \tau_0 \\ \tau_2 \end{pmatrix} + \begin{pmatrix} \sec\alpha \\ 0 \end{pmatrix}.$$

Note that $\tau_{j,n}(t)$ for $j = 0, 1, 2$ and $n \geq 1$ is a polynomial of degree $2n$ and satisfies

$$\tau_{0,n}(t) = \tau_{2,n}(1-t), \quad \tau_{1,n}(t) = 1 - \tau_{0,n}(t) - \tau_{2,n}(t), \tag{12}$$

and $\lambda_{j,n}(t)$ for $j = 0, 1, 2$ and $n \geq 0$ is a polynomial of degree $2n + 2$.

Lemma 4.1. *For all positive integers n, $\mathbf{b}_{2n}$ is a linear normal curve.*

Proof. Since

$$\begin{aligned} \lambda'_{0,n}(t) &= (1-w^2)^n(t-1)\mu_n(t) \\ \lambda'_{1,n}(t) &= (1-w^2)^n(2t-1)\mu_n(t) \\ \lambda'_{2,n}(t) &= (1-w^2)^n t\mu_n(t) \end{aligned} \tag{13}$$

we have that

$$\mathbf{b}'_{2n}(t) = \left(\sum_{i=0}^{n-1}(1-w^2)^i\mu_i(t)\right)\{(t-1)\mathbf{p}_0 + (1-2t)\mathbf{p}_1 + t\mathbf{p}_2\} \tag{14}$$

and so $\mathbf{b}_{2n}$ is a linear normal curve. □

Any point $\mathbf{x} \in \mathbb{R}^2$ can be uniquely expressed in barycentric coordinates (τ_0, τ_1, τ_2) with respect to the triangle $\mathbf{p}_0\mathbf{p}_1\mathbf{p}_2$ satisfying

$$\mathbf{x} = \sum_{j=0}^{2} \tau_j\mathbf{p}_j \quad \text{and} \quad \sum_{j=0}^{2} \tau_j = 1 \tag{15}$$

and a function $f_\mathbf{r} : \mathbb{R}^2 \to \mathbb{R}$ is defined by

$$f_\mathbf{r}(\mathbf{x}) = \tau_1^2 - 4w\tau_0\tau_2. \tag{16}$$

Then the conic $\mathbf{r}$ satisfies $f_\mathbf{r}(\mathbf{r}(t)) = 0$ [23]. The approximation curve $\mathbf{b}_{2n}$ is a G^k endpoint interpolation of the conic $\mathbf{r}$ if

$$\begin{aligned} &\mathbf{r}'(t) \cdot \mathbf{b}'_{2n}(t) > 0 && \text{for } t = 0, 1 \\ &\frac{d^i f_\mathbf{r}(\mathbf{b}_{2n}(t))}{dt^i} = 0 && \text{for } t = 0, 1 \text{ and } i = 0, 1, \ldots, k \end{aligned}$$

[13].

Proposition 4.2. *The curve* $\mathbf{b}_{2n}(t)$ *is a* G^n *endpoint interpolation of the conic* $\mathbf{r}$.

Proof. It follows from Eqs. (9), (12), and (15)–(16) that

$$f_{\mathbf{r}}(\mathbf{b}_{2n}(t)) = \tau_{1,n}(t)^2 - 4w^2\tau_{0,n}(t)\tau_{2,n}(t)$$

and it is easily checked that $f_{\mathbf{r}}(\mathbf{b}_{2n}(t)) = 0$ for all positive n and $t = 0, 1$. By Eq. (13),

$$\frac{d}{dt}f_{\mathbf{r}}(\mathbf{b}_{2n}(t)) = 2\left(\sum_{i=0}^{n-1}(1-w^2)^i\mu_i(t)\right) \cdot \left\{-(2t-1)\sum_{i=0}^{n-1}\lambda_{1,i}(t) - 2w^2\left(-(1-t)\sum_{i=0}^{n-1}\lambda_{2,i}(t) + t\sum_{i=0}^{n-1}\lambda_{0,i}(t)\right)\right\}.$$

It follows from

$$\begin{aligned}
&-(2t-1)\sum_{i=0}^{n-1}\lambda_{1,i}(t) - 2w^2(-(1-t)\sum_{i=0}^{n-1}\lambda_{2,i}(t) + t\sum_{i=0}^{n-1}\lambda_{0,i}(t))\\
&= -(2t-1)\sum_{i=0}^{n-1}(1-w^2)^n(\gamma_{n+1}(t)-\gamma_n(t)) + w^2(2t-1)\sum_{i=0}^{n-1}(1-w^2)^n\{\gamma_{n+1}(t)\}\\
&= -(2t-1)\left(1+\sum_{i=0}^{n-1}(1-w^2)^{n+1}\gamma_{n+1}(t) - (1-w^2)^n\gamma_n(t)\right)\\
&= -(2t-1)(1-w^2)^n\gamma_n(t)
\end{aligned}$$

that

$$\frac{d}{dt}f_{\mathbf{r}}(\mathbf{b}_{2n}(t)) = -2\left(\sum_{i=0}^{n-1}(1-w^2)^i\mu_i(t)\right)(2t-1)(1-w^2)^n\gamma_n(t). \tag{17}$$

Thus

$$\left.\frac{d^i}{dt^i}f_{\mathbf{r}}(\mathbf{b}_{2n}(t))\right|_{t=0,1} = 0 \qquad \text{for } i = 0, 1, \ldots, n,$$

and so $\mathbf{b}_{2n}(t)$ is a G^n endpoint interpolation of the conic $\mathbf{r}$. □

Lemma 4.3. *If any continuous curve* $\mathbf{x} : [0, 1] \to \mathbb{R}^2$ *lies in the (closed) triangle* $\triangle\mathbf{p}_0\mathbf{p}_1\mathbf{p}_2$, *then*

$$d_H(\mathbf{r}, \mathbf{x}) \le \frac{1}{4w^2}\max_{t\in[0,1]}|f_{\mathbf{r}}(\mathbf{x}(t))|\,|\mathbf{p}_0 - 2\mathbf{p}_1 + \mathbf{p}_2|.$$

(Lemma 3.2 in [13].*)*

For all weights $w < 1$, the following lemma can be proven in a manner similar to that of Lemma 3.3 since $1 - w^2 > 0$, so we omit the proof.

Lemma 4.4. *For* $w < 1$ *and all positive integers n,*

$$\sum_{i=0}^{n-1}(1-w^2)^i\mu_i(t) > 0$$

in the closed interval $[0, 1]$ *.*

Proposition 4.5. *For* $w < 1$ *and all positive n, the Hausdorff distance between the ellipse* $\mathbf{r}$ *and its approximation curve* $\mathbf{b}_{2n}$ *is bounded as*

$$d_H(\mathbf{r}, \mathbf{b}_{2n}) \le \frac{1}{4w^2}|\mathbf{p}_0 - 2\mathbf{p}_1 + \mathbf{p}_2|\left(1-(1+w)\sum_{i=0}^{n-1}\frac{\binom{2i}{i}}{i+1}\frac{(1-w^2)^i}{2^{2i+1}}\right) \cdot \left(1-(1-w)\sum_{i=0}^{n-1}\frac{\binom{2i}{i}}{i+1}\frac{(1-w^2)^i}{2^{2i+1}}\right), \tag{18}$$

and its approximation order is $2n + 2$.

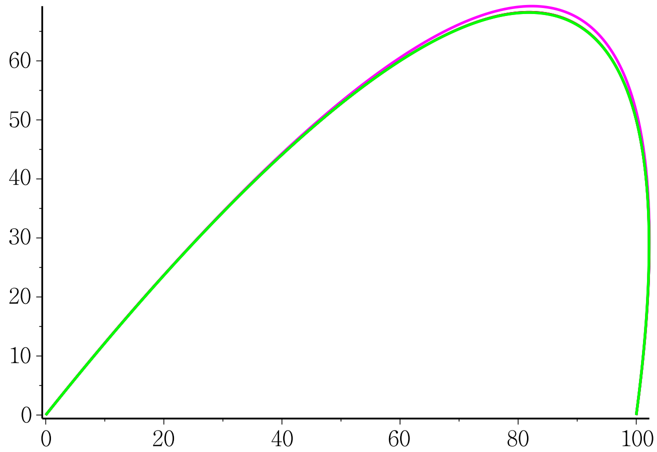

Fig. 3. The ellipse **r** (green), quartic approximation curves using the methods of Kovač and Žagar [24] (black), Hu [25] (red) and [26] (blue), our method (magenta), and the quintic approximation curve (khaki) by Floater [13]. (For interpretation of the references to color in this figure legend, the reader is referred to the web version of this article.)

Proof. By Eq. (14) and Lemma 4.4, for all positive integers n and weights $w < 1$,

$$0 \leq \tau_{0,n}(t), \tau_{1,n}(t), \tau_{2,n}(t) \leq 1.$$

Thus for all positive integers n and ellipse $\mathbf{r}$, $\mathbf{b}_{2n}$ is contained inside of the (closed) triangle $\mathbf{p}_0\mathbf{p}_1\mathbf{p}_2$. By Eq. (17) and Lemma 4.3, $f_{\mathbf{r}}(\mathbf{b}_{2n}(t))$ is increasing in $[0, \frac{1}{2}]$ and decreasing $[\frac{1}{2}, 1]$, and $f_{\mathbf{r}}(\mathbf{b}_{2n}(t)) \geq 0$ for all $t \in [0, 1]$. Thus $\mathbf{b}_{2n}$ lies outside the ellipse $\mathbf{r}$. Since $\max_{t\in[0,1]}|f_{\mathbf{r}}(\mathbf{b}_{2n}(t))| = f_{\mathbf{r}}(\mathbf{b}_{2n}(\frac{1}{2}))$ and

$$\lambda_{0,n}(1/2) = \frac{1}{2}\lambda_{1,n}(1/2) = \lambda_{2,n}(1/2) = \frac{\binom{2n}{n}}{n+1}\frac{(1-w^2)^n}{2^{2n+2}} \tag{19}$$

for $n = 0, 1, \ldots,$ we have

$$f_{\mathbf{r}}(\mathbf{b}_{2n}(1/2)) = \left(1 - \sum_{i=0}^{n-1}\frac{\binom{2i}{i}}{i+1}\frac{(1-w^2)^i}{2^{2i+1}}\right)^2 - w^2\left(\sum_{i=0}^{n-1}\frac{\binom{2i}{i}}{i+1}\frac{(1-w^2)^i}{2^{2i+1}}\right)^2$$

and Eq. (18) follows. By Taylor series expansion

$$\frac{1}{1+\sqrt{1-x}} = \sum_{n=0}^{\infty}\frac{\binom{2n}{n}}{n+1}\frac{x^n}{2^{2n+1}},$$

we have

$$1 - (1+w)\sum_{i=0}^{n-1}\frac{\binom{2i}{i}}{i+1}\frac{(1-w^2)^i}{2^{2i+1}} = \mathcal{O}((1-w)^n).$$

Since $1 - w$ and $|\mathbf{p}_0 - 2\mathbf{p}_1 + \mathbf{p}_2|$ are $\mathcal{O}(s^2)$ (refer to [13]), $d_H(\mathbf{r}, \mathbf{b}_{2n}) = \mathcal{O}(s^{2n+2})$, where s is the arc-length of the ellipse. □

5. Comparison to previous methods of ellipse approximation

In this section, we present an example to compare our approximation method to the previous approximation methods. The example consists of an ellipse given by quadratic rational Bézier curve $\mathbf{r}(t)$ (green color) with the control points (0, 0), (150, 120), (100, 0) which was used by Kovač and Žagar [24] and Hu [25]. This conic has the weight $w = \frac{5}{6}$, and is illustrated in Fig. 3.

Floater [13] presented a conic approximation method using G^{n-1} spline curves of any odd degree n with approximation order $2n$. The quintic approximation curve (khaki color) using that method for the given ellipse $\mathbf{r}$ has an upper bound of Hausdorff distance 9.73×10^{-5}, as seen in Fig. 3.

Kovač and Žagar [24] presented a quartic G^1 endpoint interpolation of conic for the weight w satisfying $\sqrt{4\sqrt{2}-5} < w < \sqrt{2\sqrt{2}-1}$, and that method yields a f quartic approximation (black color) of the given ellipse with an upper bound of the Hausdorff distance 4.37×10^{-2}. Hu [25] found another quartic G^1 endpoint interpolation (red color) of conic whose upper bound is 3.56×10^{-4}, as shown in Fig. 3.

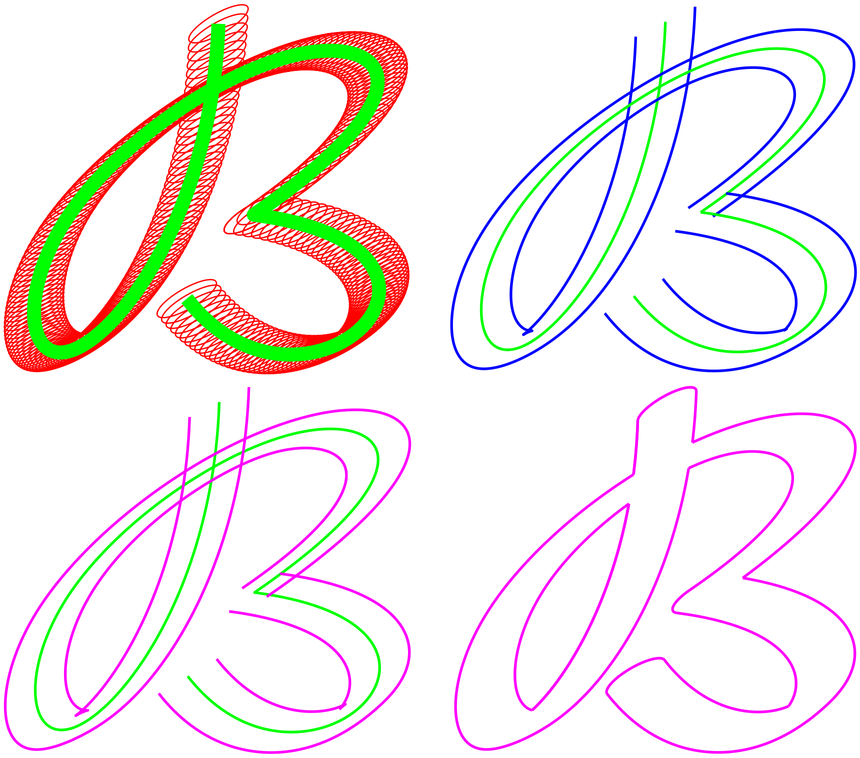

Fig. 4. Upper left: the skeleton curve (green) **q** and ellipses (red) **r**. Upper right: the convolution curve (blue) $\mathbf{q} * \mathbf{r}$. Lower left: the convolution curve (magenta) $\mathbf{q} * \mathbf{b}_2$. Lower right: the trimmed curve. (For interpretation of the references to color in this figure legend, the reader is referred to the web version of this article.)

The approximation method by Hu [26] gives the best L_2 approximation of a conic by G^1 Bézier curves of any degree n. For the given ellipse, the quartic approximation curve (blue color) has the L_2 distance 4.53×10^{-2} in Fig. 3.

Our method yields a G^n endpoint interpolation of the ellipse by LN Bézier curves of any even degree $2n$ with the upper bound of the Hausdorff distance given in Eq. (18). Fig. 3 shows the quartic Bézier curve (magenta color) whose upper bound of the Hausdorff distance is 1.44.

Our LN Bézier approximation is not as tight as the other approximation curves. For instance, in Fig. 3 the other approximation curves cannot be visually distinguished from the original ellipse. However, our LN Bézier approximation has the merit that it yields a rational offset, which is not the case for any of the other methods.

6. Application

In this section we present an application of our approximation method. The application consists of the approximation of the convolution curves of a spline curve and of ellipses. Only our method of LN approximation of ellipses can yield the rational offsets. The other methods that were compared in the previous section cannot.

As shown in Fig. 4, the LN ellipse approximation $\mathbf{b}_2$ of degree four can be used to approximate the boundaries of a Minkowski sum, here the outline of the letter "B" in some font. (For more information about Minkowski sums we refer to [27–29].)

An ellipse **r** (red color) whose long and short axes lengths are 2 and 0.6 units, respectively, moves along a skeleton curve **q** (green color) which is C^2 continuous except for one cusp and is composed of five cubic Bézier curves with the control points

$(7.344, 9.756)$, $(7.164, 4.32)$, $(4.572, .774)$, $(3.126, .135)$, $(1.68, -.504)$, $(1.38, 1.764)$, $(2.88, 4.026)$, $(4.38, 6.288)$, $(7.68, 8.544)$, $(10.005, 8.907)$, $(12.33, 9.27)$, $(13.68, 7.74)$, $(8.388, 4.104)$, $(16.128, 3.096)$, $(9.9, -2.88)$, and $(6.408, 1.62)$.

The boundaries of Minkowski sums can be obtained from the convolution curve $\mathbf{q} * \mathbf{r}$ (blue color) of the two curves **q** and **r** [27], which is not a rational curve. Using our method for the G^2 quartic LN approximation $\mathbf{b}_2$ of the ellipse, we obtain the convolution curve $\mathbf{q} * \mathbf{b}_2$ (magenta color) which approximates $\mathbf{q} * \mathbf{r}$, the outline of font B. Since the curve **q** is C^2-continuous except for one cusp, the approximation curve $\mathbf{q} * \mathbf{b}_2$ is G^2-continuous except for cusps and discontinuous points, as shown in Fig. 4. Since $\mathbf{b}_2$ is a quartic LN curve, the convolution $\mathbf{q} * \mathbf{b}_2$ is a rational curve of degree eleven. Finally, the outline of font (magenta color) can be obtained by the trimming curve $\mathbf{q} * \mathbf{b}_2$, as shown in Fig. 4.

7. Summary and conclusion

In this paper we found a sequence of LN curves $\mathbf{b}_{2n}$ of degree $2n$ which are G^n endpoint interpolations of a circular arc and have approximation order $2n+2$. We presented an extension of the circle approximation to the ellipse approximation by G^n LN curves $\mathbf{b}_{2n}$ of degree $2n$, and obtained the Hausdorff distance $d_H(\mathbf{r}, \mathbf{b}_{2n})$ between the ellipse $\mathbf{r}$ and the LN curve $\mathbf{b}_{2n}$. We also illustrated that the G^n approximation of the convolution curves of ellipses and a spline curve can be obtained in rational form using our method of G^n LN ellipse approximation.

Acknowledgments

This study was supported by research funds from Chosun University, South Korea, 2017. The authors are very grateful to two anonymous reviewers for their valuable comments and constructive suggestions.

References

[1] C. de Boor, M. Sabin, High accuracy geometric Hermite interpolation, Comput. Aided Geom. Des. 4 (1987) 269–278.
[2] T. Dokken, M. Dæhlen, T. Lyche, K. Mørken, Good approximation of circles by curvature-continuous Bézier curves, Comput. Aided Geom. Des. 7 (1990) 33–41.
[3] K. Mørken, Best approximation of circle segments by quadratic Bézier curves, in: P.J. Laurent, A. Le Méhauté, L.L. Schumaker (Eds.), Curves and Surfaces, Academic Press, 1990, pp. 387–396.
[4] M. Goldapp, Approximation of circular arcs by cubic polynomials, Comput. Aided Geom. Des. 8 (1991) 227–238.
[5] T. Dokken, Aspects of Intersection Algorithms and Approximation (Ph.D. thesis), University of Oslo, 1997.
[6] Y.J. Ahn, H.O. Kim, Approximation of circular arcs by Bézier curves, J. Comput. Appl. Math. 81 (1997) 145–163.
[7] L. Fang, Circular arc approximation by quintic polynomial curves, Comput. Aided Geom. Des. 15 (1998) 843–861.
[8] L. Fang, G^3 approximation of conic sections by quintic polynomial, Comput. Aided Geom. Des. 16 (1999) 755–766.
[9] T. Dokken, Controlling the shape of the error in cubic ellipse approximation, in: Curve and Surface Design, Nashboro Press, Saint-Malo, 2002, pp. 113–122.
[10] S.H. Kim, Y.J. Ahn, Approximation of circular arcs by quartic Bézier curves, Comput.-Aided Des. 39(6) (2007) 490–493.
[11] Y.J. Ahn, Approximation of conic sections by curvature continuous quartic Bézier curves, Comput. Math. Appl. 60 (2010) 1986–1993.
[12] M. Floater, High-order approximation of conic sections by quadratic splines, Comput. Aided Geom. Des. 12(6) (1995) 617–637.
[13] M. Floater, An $O(h^{2n})$ Hermite approximation for conic sections, Comput. Aided Geom. Des. 14 (1997) 135–151.
[14] I.-K. Lee, M.-S. Kim, G. Elber, Planar curve offset based on circle approximation, Comput.-Aided Des. 28 (1996) 617–630.
[15] W. Lü, Rational offsets by reparametrizations, preprint, 1992.
[16] R.T. Farouki, T.W. Sederberg, Analysis of the offset to a parabola, Comput. Aided Geom. Des. 12 (6) (1995) 639–645.
[17] B. Jüttler, Triangular Bézier surface patches with a linear normal vector field, in: R. Cripps, editor, The Mathematics of Surfaces VIII, Information Geometers, pp. 431–446, Winchester, 1998.
[18] Y.J. Ahn, C.M. Hoffmann, Circle approximation using LN Bézier curves of even degree and its application, J. Math. Anal. Appl. 40 (2014) 257–266.
[19] Y.J. Ahn, C.M. Hoffmann, Y.S. Kim, Curvature-continuous offset approximation based on circle approximation using quadratic Bézier biarcs, Comput.-Aided Des. 43 (2011) 1011–1017.
[20] S.W. Kim, S.C. Bae, Y.J. Ahn, An algorithm for G^2 offset approximation based on circle approximation by G^2 quadratic spline, Comput.-Aided Des. 73 (2016) 36–40.
[21] J.A. Gregory, Geometric continuity, in: T. Lyche, L. Schumaker (Eds.), Mathematical Methods in CAGD, Academic Press, 1989, pp. 353–371.
[22] M. Sampoli, M. Peternell, B. Jüttler, Rational surfaces with linear normals and their convolutions with rational surfaces, Comput. Aided Geom. Des. 23 (2006) 179–192.
[23] G. Farin, Curves and Surfaces for CAGD, Morgan-Kaufmann, San Francisco, 2002.
[24] B. Kovač, E. Žagar, Some new G^1 quartic parametric approximants of circular arcs, Appl. Math. Comput. 239 (2014) 254–264.
[25] Q.Q. Hu, G^1 approximation of conic sections by quartic Bézier curves, Comput. Math. Appl. 68 (2014) 1882–1891.
[26] Q.Q. Hu, Explicit G^1 approximation of conic sections using Bézier curves of arbitrary degree, J. Comput. Appl. Math. 292 (2016) 505–512.
[27] I.-K. Lee, M.-S. Kim, G. Elber, Polynomial/Rational Approximation of Minkowski sum boundary curves, Graph Models Image Process. 60 (1998) 136–165.
[28] J.-H. Lee, S.J. Hong, M.-S. Kim, Polygonal boundary approximation for a 2D general sweep based on envelope and boolean operations, Vis. Comput. 16 (2000) 208–240.
[29] R.T. Farouki, J. Hass, Evaluating the boundary and covering degree of planar Minkowski sums and other geometrical convolutions, J. Comput. Appl. Math. 209 (2007) 246–266.